

# Absolute frequency measurement of the iodine-stabilized He–Ne laser at 633 nm

T.H. Yoon<sup>1,\*</sup>, J. Ye<sup>1,\*\*</sup>, J.L. Hall<sup>1,\*\*</sup>, J.-M. Chartier<sup>2</sup>

<sup>1</sup>JILA, University of Colorado and National Institute of Standards and Technology, Boulder, CO 80309-0440, USA

<sup>2</sup>Bureau International des Poids et Mesures, Pavillon de Breteuil, 92312 Sèvres Cedex, France

Received: 29 May 2000/Revised version: 13 September 2000/Published online: 22 November 2000 – © Springer-Verlag 2000

**Abstract.** The absolute frequency of an iodine-stabilized He–Ne laser at 633 nm stabilized on the *i* (or  $a_{13}$ ) component of the 11-5 R(127) hyperfine transition of the  $^{127}\text{I}_2$  molecule is measured using a femtosecond optical comb generator and an iodine-stabilized Nd:YAG laser standard at 1064 nm. We link the measured absolute frequency to the current internationally adopted value via frequency intercomparison between JILA and the Bureau International des Poids et Mesures (BIPM), leading to the determination of the absolute frequency of the BIPM-4 standard laser. The resulting absolute frequency  $f_{i(\text{BIPM})}$  of the BIPM-4 standard laser is  $f_{i(\text{BIPM})} = 473\,612\,214\,711.9 \pm 2.0$  kHz, which is 6.9 kHz higher than the value adopted by the Comité International des Poids et Mesures (CIPM) in 1997.

**PACS:** 06.20.-f; 06.20.Fn; 06.30.Bp

Precise measurement of an optical frequency in the visible region of the spectrum is important in metrology as well as in many fundamental applications such as precision spectroscopy and the determination of fundamental physical constants. In metrology, the definition of the unit of length and its practical realization are based on both the adopted value for the speed of light in vacuum,  $c = 299\,792\,458$  m/s, and the frequency of an optical frequency standard. Thus, length measurements can be now linked to the unit of time. Among the listed optical frequency standards recommended by the Comité International des Poids et Mesures (CIPM) in 1997 [1], the iodine-stabilized He–Ne laser at 633 nm takes a unique position in that it has been used most widely for calibrating lasers used in metrology and therefore has been the objective of frequency intercomparisons between many

national metrology institutes. Although there have been extensive efforts to establish the frequency reproducibility of the system through heterodyne frequency comparisons between metrology laboratories [2], it has been very difficult to measure the frequency accuracy of the system, i.e., the absolute frequency determination based on a phase coherent frequency chain linked to a Cs primary clock, the current realization of the unit of time. Acef et al. [3] measured the absolute frequency of an iodine-stabilized He–Ne laser at 633 nm by using a  $10\ \mu\text{m}$   $\text{CO}_2$  laser to link to a visible optical-frequency synthesis chain. The recommended value of the frequency adopted by the CIPM in 1997 was based on that measurement. The current frequency value of the component *i* (or  $a_{13}$ ) of the absorbing molecule  $^{127}\text{I}_2$ , transition 11-5 R(127), is  $f_{i(\text{CIPM})} = 473\,612\,214\,705$  kHz  $\pm 12$  kHz, corresponding to a relative standard uncertainty of  $2.5 \times 10^{-11}$ , for the standard laser operating conditions listed in [1].

Quite recently, it was demonstrated that Kerr-lens mode-locked femtosecond lasers can be used to measure the absolute frequency of an optical frequency standard based on a narrow transition of an atom, ion, or molecule [4–9]. In those experiments the repetition rate (or mode spacing of the comb) of the femtosecond laser was locked phase-coherently to the microwave frequency standard, the primary atomic Cs clock. Use of the femtosecond comb generator (FCG) drastically simplifies the frequency measurement scheme, moving from a complicated traditional frequency synthesis chain to a reliable and compact table-top FCG system. Therefore, it is important for metrology to apply this new approach and its associated enhancement of measurement accuracy in the determination of the absolute frequency of an iodine-stabilized He–Ne laser at 633 nm.

In this paper we apply the FCG technique to measure the absolute frequency of the *i* (or  $a_{13}$ ) component of the 11-5 R(127) hyperfine transition of the  $^{127}\text{I}_2$  molecule at 633 nm. By comparing the frequencies of portable iodine-stabilized He–Ne lasers between JILA and the Bureau International des Poids et Mesures (BIPM), we determine the frequency of the *i* component of the BIPM-4 standard laser, which serves

\*Corresponding author.

Permanent address: Korea Research Institute of Standards and Science, 1 Toryong, Yusong, Taejon 305-600, Korea  
(E-mail: thyoona@kriss.re.kr)

\*\*Staff member, Quantum Physics Division, National Institute of Standards and Technology, Boulder, CO 80303, USA

as the as-maintained international iodine-stabilized He–Ne laser standard at 633 nm. It should be noted that the portable lasers used for determination of the absolute frequency of the BIPM-4 standard laser are transfer flywheels to link the absolute values measured at JILA to those of the BIPM. The transfer lasers are well-evolved commercial units whose robustness and stability are well suited to this task. This is, to our knowledge, the first systematic study to determine the absolute frequency of the international iodine-stabilized He–Ne laser standard at 633 nm by using a FCG technique. The optical frequency is determined by the current FCG setup at JILA with a statistical coherence and apparent accuracy of about  $2 \times 10^{-12}$ , or 600 Hz.

## 1 Frequency comparison of two iodine-stabilized He–Ne lasers

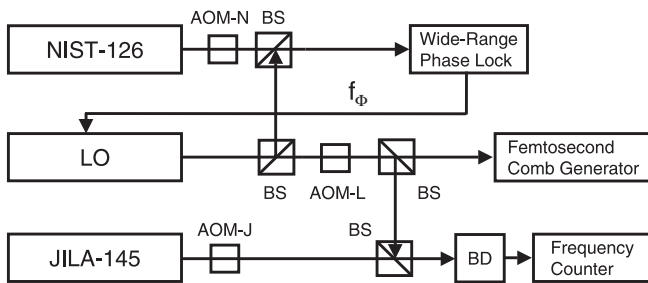
Before making the absolute frequency measurement, we first measured the frequency difference between two iodine-stabilized He–Ne lasers, one of which would then be used for the frequency intercomparison. In the experiment, two commercial iodine-stabilized He–Ne lasers (NIST-126 and JILA-145) and one high-power modulation-free local oscillator (LO), which was phase locked to the NIST-126 laser with fixed frequency offset  $f_\phi$ , are employed as shown in Fig. 1a. The NIST-126 laser remained operating in the laboratory during the entire intercomparison period, while the JILA-145 laser was transported to the National Research Council of Canada (NRC) in Ottawa for the frequency intercomparison with two other portable lasers of the BIPM and the NRC. Since the LO contains no modulation in its spectrum, we explored the beat spectra between the LO and either the NIST-126 or the JILA-145 laser separately to accurately measure the frequency-modulation (FM) amplitudes (widths) as described below. Use of the LO in this manner also facilitates measurement of the frequency difference between the two iodine-stabilized He–Ne lasers, since they are

unaffected by the modulated output spectrum of each other. To achieve good isolation from the back-reflected beams, an acousto-optic modulator was placed at the output of each laser as shown in Fig. 1a by AOM-N, AOM-L, and AOM-J. The measured frequencies  $f_{\text{AOM-N}}$ ,  $f_{\text{AOM-L}}$ , and  $f_{\text{AOM-J}}$  associated with AOM-N, AOM-L, and AOM-J are listed in Table 1, together with the phase-lock offset frequency  $f_\phi$ . The introduced frequency offsets of the LO, the JILA-145 laser, and the NIST-126 laser, after passing through their AOMs, are  $+f_{\text{AOM-L}}$  ( $+1^{\text{st}}$  order) and  $-f_{\text{AOM-J}}$  ( $-1^{\text{st}}$  order), and  $-2 \times f_{\text{AOM-N}}$  ( $-1^{\text{st}}$  order double-passed), respectively, with respect to their laser output frequencies. The factor of two arises for the NIST-126 laser because we double-passed the AOM-N. This latter configuration is attractive for use with the “anti-dither” concept to actively cancel the frequency modulated spectrum by applying an accurately matching negative version of the He–Ne laser’s FM dither to the AOM [10]. Frequency relations among the NIST-126 laser, the JILA-145 laser, and the LO in Fig. 1a are summarized in Fig. 1b.

To determine precisely any frequency shifts that might have happened during the trip for the frequency intercomparison, we performed a systematic investigation of the coefficients of the frequency shifts, such as iodine-cell temperature, laser output power, and peak-to-peak FM amplitude, for the JILA-145 laser under different laser operating conditions. We studied the effect of these operating parameters on the fre-

**Table 1.** Measured frequencies associated with AOM-N, AOM-L, AOM-J, and  $f_\phi$  in Fig. 1a:  $f$  is the corresponding frequency and  $s$  is the estimated standard uncertainty for one measurement

	$f$ (MHz)	$s$ (Hz)
$f_{\text{AOM-N}}$	79.999686	0.3
$f_{\text{AOM-L}}$	79.999237	0.2
$f_{\text{AOM-J}}$	80.002866	0.2
$f_\phi$	193.624679	3.0



**a**

$$f_{\text{NIST-126}} = f_{\text{LO}} + f_\phi + 2f_{\text{AOM-N}}$$

$$f_{\text{JILA-145}} = f_{\text{LO}} + f_{\text{AOM-L}} + f_{\text{BD}} + f_{\text{AOM-J}} = f_{\text{FCG}} + f_{\text{BD}} + f_{\text{AOM-J}}$$

**b**

**Fig. 1.** **a** Schematic of the experimental setup used to measure the frequency difference between two iodine-stabilized He–Ne lasers, NIST-126 and JILA-145, at 633 nm. Components shown are local oscillator (LO), acousto-optic modulators (AOM), beam splitter (BS), beat frequency detector (BD), and phase-lock frequency ( $f_\phi$ ). **b** Frequency relations among the NIST-126 laser, the JILA-145 laser, and the LO in **a**

**Table 2.** Effects of modulation amplitude, iodine temperature, and output power on the measured frequencies of the d, e, f, and g components of the transition 11-5 R(127) of  $^{127}\text{I}_2$  for the JILA-145 laser.  $L$  is the slope of a linear fit to the data points and  $u$  is the standard deviation for one measurement

Operating parameters	Component	$L$	$u$
Iodine-cell temperature coefficient ( $\Delta f/\Delta\theta_{\text{I}_2}$ )(kHz/K)	d	−13.23	0.20
	e	−13.21	0.30
	f	−12.55	0.27
	g	−13.16	0.20
	h	−13.53	0.74
	i	−13.67	0.18
FM amplitude coefficient ( $\Delta f/f_w$ )(kHz/MHz)	Average	−13.23	0.31
	d	−6.26	1.18
	e	−10.52	0.60
	f	−9.43	0.83
	g	−13.20	0.38
Extracavity power coefficient ( $\Delta f/\Delta P$ )(kHz/ $\mu\text{W}$ )	Average	−9.86	0.75
	d	+0.004	0.020
	e	−0.080	0.014
	f	−0.095	0.021
	g	−0.124	0.022
	Average	−0.074	0.019

quency shift of four hyperfine components, d (or  $a_{18}$ ), e (or  $a_{17}$ ), f (or  $a_{16}$ ), and g (or  $a_{15}$ ). The schematic of the experiment is again shown in Fig. 1a and the measurement results are summarized in Table 2. (The iodine-temperature dependence of the h (or  $a_{14}$ ) and i (or  $a_{13}$ ) components was also measured and is included in Table 2.) In addition, the intensity transmittance of the output coupler of the JILA-145 laser was measured to be  $7.8 \times 10^{-3}$ , and so the recommended one-way intracavity power of 10 mW would be satisfied at an output power of  $78 \mu\text{W}$ .

For the measurement of the FM amplitude in Table 2, we employed a frequency-to-voltage (F/V) converter and a fast-Fourier-transform (FFT) spectrum analyzer. To use this system for the analysis of laser beat spectrum, we down-mixed the detected beat frequency with a stable radio-frequency (RF) synthesizer. The calibration tests were performed at the frequency of 20 MHz from the RF Mixer, which was the central operating frequency of the F/V converter. The schematic of this experiment is shown in Fig. 2, where the beat detector corresponds to the beat detector BD in Fig. 1a. We measured the FM amplitude under conditions where the JILA-145 laser was either locked or unlocked, with no discernible differences. Using a digitally precise frequency synthesizer with FM capability, we confirmed that this measurement technique has the accurate dither calibration of  $3.00 \pm 0.015$  V peak-to-peak for a 6 MHz peak-to-peak FM span at the 8.333 kHz dither frequency. The F/V distortion was small, with the largest harmonic being the 2<sup>nd</sup>, at  $-70$  dB relative to the fundamental.<sup>1</sup>

We measured the 16 elements of the  $4 \times 4$  matrix for the frequency difference between each of the d, e, f, and

<sup>1</sup>This F/V design uses a charge-pump concept, transferring a rate-independent charge quantum for each positive-going zero-crossing of its input wave.

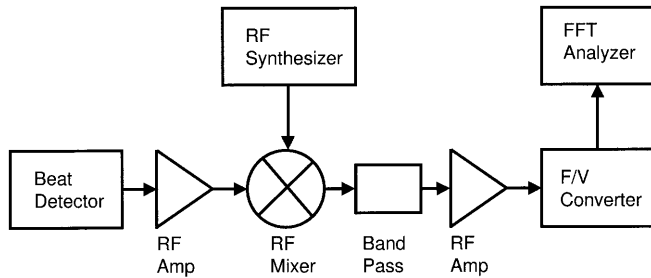


**Fig. 2.** Experimental setup used to measure the FM amplitude with a frequency-to-voltage converter and an FFT spectrum analyzer

**Table 3.** Average frequency difference  $\Delta f$  with standard deviation  $s$  between the JILA-145 and the NIST-126 lasers before and after frequency intercomparison, where  $\theta_2$ ,  $f_w$ , and  $P$  are the iodine-cell temperature, the peak-to-peak FM amplitude, and the output power of the JILA-145 laser when the frequency is stabilized on the d component. Values for the NIST-126 laser were kept constant during the whole experiment at  $14.88^\circ\text{C}$ ,  $6.0$  MHz, and  $85 \mu\text{W}$ , respectively

$f_{\text{JILA-145}} - f_{\text{NIST-126}}$	$\Delta f$ (kHz)	$s$ (kHz)	$\theta_2$ ( $^\circ\text{C}$ )	$f_w$ (MHz)	$P$ ( $\mu\text{W}$ )
Before	1.0	1.1	14.91	5.67	98
After	-1.8	0.7	14.91	5.98	92

g components of the NIST-126 and the JILA-145 lasers to determine the average frequency difference between the two systems before and after the frequency intercomparison. From these measurements we also obtained the frequency intervals between each hyperfine component. Table 3 shows the results for the average frequency difference between the NIST-126 and JILA-145 laser systems both before and after the frequency intercomparison. The operating parameters, such as iodine-cell temperature, FM amplitude, and laser output power, for the NIST-126 laser were kept constant at the values of  $14.88^\circ\text{C}$ ,  $6.0$  MHz, and  $85 \mu\text{W}$  during the whole experiment. As may be seen in Table 3, there was an apparent change of average frequency difference between the JILA-145 and NIST-126 lasers from  $+1.0$  kHz to  $-1.8$  kHz, which can be clearly understood by considering the deliberate operating-parameter changes of the JILA-145 laser midway through the JILA-BIPM frequency intercomparison. Namely, it was judged useful to modify the power and FM dither settings of the JILA-145 laser to better match the conditions set forth in the CIPM documentation [1]. Using the coefficients of frequency shift given in Table 2, we found that a modulation amplitude change of  $+0.31$  MHz shifts the “before” frequency of the JILA-145 laser down by  $-3.1$  kHz, while an output-power change of  $6 \mu\text{W}$  shifts the “before” frequency of the JILA-145 laser up by  $0.4$  kHz. The total frequency shift induced by the operating-parameter changes is thus about  $-2.7$  kHz, which accounts nearly completely for the apparent frequency change of about  $-2.8$  kHz between the “before” and “after” measurements. This is the basis for our confidence that the transport process had no significant effect on the frequency reproducibility of by the JILA-145 laser.

## 2 Absolute frequency measurement using femtosecond optical comb generator

Figure 3 shows the experimental setup that we used to measure the absolute frequency of the 633 nm He-Ne laser; we used an FCG and an iodine-stabilized Nd:YAG laser at either 532 nm or the laser’s fundamental frequency of 1064 nm. The details of the experimental setup for the FCG are published elsewhere [8]. The absolute frequency of the 1064 nm

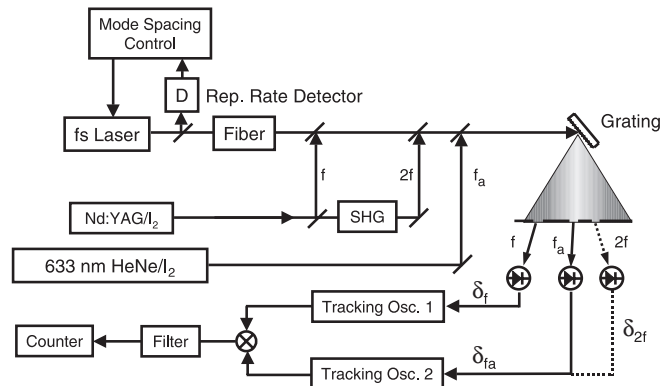


**Fig. 3.** Experimental setup used to measure the absolute frequency of 633 nm He-Ne laser with a femtosecond comb generator and an iodine-stabilized Nd:YAG laser at 1064 nm

Nd:YAG frequency standard, stabilized to the  $a_{10}$  component of the 32-0 R(56) hyperfine transition of  $^{127}\text{I}_2$ , is reported to be  $f = 281\,630\,111\,757.20 \pm 0.65$  kHz [8]. It is worthwhile to note the stability of our FCG system: each time we measure an unknown frequency, for example  $f_a$  in Fig. 3, we measure the absolute frequency of the iodine-stabilized Nd:YAG laser at either 1064 nm or 532 nm. In this 4-month record of the absolute frequency measurements, we found that the measured day-to-day values agreed to within  $\pm 0.5$  kHz at 1064 nm. We also note that because we measure the absolute frequency of the Nd:YAG laser before each measurement of  $f_a$ , only the stability of the iodine-stabilized Nd:YAG system, and not its larger realization uncertainty, is relevant to the absolute frequency measurement of  $f_a$  [8].

In Fig. 3,  $\delta_f$  ( $\delta_{2f}$ ) is the beat frequency between the 1064 (532) nm Nd:YAG laser, whose frequency is stabilized to the  $a_{10}$  component of the 32-0 R(56) transition at 532 nm, and the nearest comb component, while  $\delta_{f_a}$  is the beat frequency between the 633 nm He–Ne laser and the nearest comb component. Therefore, the unknown frequency  $f_a$  in Fig. 3 can be determined by counting the beat frequencies  $\delta_f$  (or  $\delta_{2f}$ ) and  $\delta_{f_a}$  between the nearest comb components at  $f$  (or  $2f$ ) and  $f_a$ , respectively.

We measure the absolute frequency of the  $i$  component of the 11-5 R(127) hyperfine transition of  $^{127}\text{I}_2$  for the JILA-145 laser in two steps. First, the output of the LO passing through the AOM-L, whose fundamental frequency is phase-locked to the  $i$  component of the NIST-126 laser in Fig. 1a, is sent to the  $f_a$  port in Fig. 3 for measurement of the absolute frequency ( $f_{\text{FCG}}$  in Fig. 1b). Since the signal-to-noise ratio (S/N) of the heterodyne beat signals at both the red and infrared portions of the spectrum is typically  $\sim 15$  to 20 dB in a 100 kHz bandwidth, which is insufficient for accurate direct counting, we use tracking oscillators in each channel. Second, on the same day, we measure the frequency

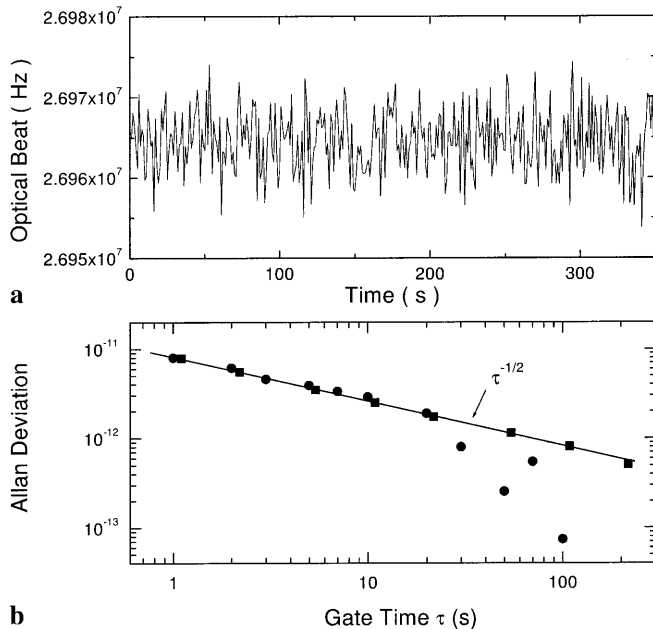


**Fig. 4.** **a** Measurement of the sum of the beat frequencies,  $\delta_{f_a} + \delta_f$  in Fig. 3, with a gate time of 1 s. **b** Allan deviation corresponding to **a**

difference between the LO beam and the JILA-145 laser by heterodyne beat, as shown in Fig. 1a ( $f_{\text{BD}}$  in Fig. 1b). The parameters of the JILA-145 laser continue to be set to the “after” values in Table 3. The measured beat frequency  $f_{\text{BD}}$  between the LO after AOM-L and the JILA-145 laser after AOM-J, when both the NIST-126 and the JILA-145 lasers are locked on the  $i$  components, is  $f_{\text{BD}} = 193\,619.24 \pm 1.00$  kHz.

Figure 4a shows the typical beat frequency as a function of time with an average (gate) time  $\tau$  of 1 s corresponding to the sum of the beat frequencies  $\delta_f$  and  $\delta_{f_a}$ . By measuring the sum or difference frequencies of the  $\delta_f$  and  $\delta_{f_a}$ , we can effectively eliminate the common-mode noise problem, which arises from fluctuations of the carrier frequency offset of the fs mode-locked laser [8]. Figure 4b shows the Allan deviation corresponding to the measurement of the sum of the beat frequencies in Fig. 4a (solid circles ●), together with the Allan deviation of the JILA-145 laser from the manufacturer’s data (solid squares ■). The straight line in Fig. 4b is a visual guide indicating  $\tau^{-1/2}$  dependence of the Allan deviation with the averaging time  $\tau$ . It is clear from Fig. 4b that the measurement uncertainty of the current FCG system is not limited by the FCG measurement system itself; rather, it is limited by the stability of the iodine-stabilized He–Ne laser. It often happened that for  $\tau \geq 30$  s the Allan deviation became even smaller than that expected for the JILA-145 laser: we offer no explanation, but note this drop-off behavior does occur beyond the time scale of some periodic perturbation process.

The repetition rate of the femtosecond laser is locked to a local Rb clock whose frequency is accurately known relative to the NIST primary Cs clock via a common-view GPS link [8]. For the data presented here, the repetition rate is 100 013.720 kHz and the number of comb mode-spacings between  $f_a$  and  $f$  is 1 919 555. We know the absolute value of  $f = 281\,630\,111\,757.22 \pm 0.30$  kHz for the iodine-stabilized Nd:YAG laser at 1064 nm, which was measured on the same day as our He–Ne measurements and is consistent with our recently published value [8]. We find the frequency of the  $i$  component at the frequency input port of the femtosecond comb generator in Fig. 1a (or  $f_{\text{FCG}}$  in Fig. 1b) to be  $f_{\text{FCG}} = 473\,611\,941\,089.84 \pm 0.31$  kHz. We apply frequency correction of  $-0.38$  kHz for the measured frequency to the standard operating conditions (10 mW one-way intracavity power, 15 °C cold-finger temperature, and 6 MHz peak-to-peak FM width; recommended by the CIPM [1]) by using the average coefficients in Table 2 for the ‘after’ values in Table 3. From the frequency relations between  $f_{\text{FCG}}$  and  $f_{\text{JILA-145}}$  in Fig. 1b, we obtain the following absolute frequency  $f_{i(\text{JILA})}$  for the  $i$  component of the 11-5 R(127) hyperfine transition of the  $^{127}\text{I}_2$  molecule of the JILA-145 laser:

$$f_{i(\text{JILA})} = 473\,612\,214\,711.57 \pm 1.06 \text{ kHz}. \quad (1)$$

Ultimately the measurement uncertainty for the absolute measurement of an optical frequency by using the FCG system arises from the environmental sensitivity in our present Rb-based atomic RF reference system: reaching the interesting transfer accuracy  $< 10^{-13}$  requires 24 h averaging of the common-view GPS data. The measured absolute frequency is 6.6 kHz higher than the internationally adopted values in 1997 [1]. We also measure the absolute frequency of the

f component of the JILA-145 laser that results in the frequency interval  $\Delta(f_f - f_i)$  between the f and i components to be 138 890.80 kHz, which agrees well with the value of 138 891.00 kHz measured by the heterodyne measurement set-up in Fig. 1.

### 3 Frequency comparison between JILA and BIPM

It is important to link the absolute frequency of the JILA-145 laser measured in the present work to the frequency of the BIPM-4 standard laser, since the absolute frequency of the BIPM-4 laser is known [3] and the current practical realization of the definition of the meter, adopted by the CIPM in 1997, is based on that value [1]. The JILA-145 and BIPM-P3 lasers were transported to the NRC in Ottawa, Canada, for a frequency intercomparison. From April 10 to 14, 2000, we performed frequency intercomparisons between the BIPM, NRC, and JILA lasers as well as an absolute frequency measurement of an iodine-stabilized He–Ne laser at 633 nm (f component of the INMS-3 laser of the NRC) by using the phase-coherent NRC frequency synthesis chain and the  $\text{Sr}^+$  optical frequency standard.

We emphasize the role of the JILA-145 and BIPM-P3 lasers as being transfer flywheels for the determination of the absolute frequency of the BIPM-4 standard laser; namely, we measured the frequency interval between the JILA-145 and BIPM-4 lasers via the BIPM-P3 laser, and then measured the absolute frequency of the JILA-145 laser under the same operating conditions, from which we obtained the absolute frequency of the BIPM-4 standard laser.

The average frequency differences among the three standard lasers participating in the frequency determination of the BIPM-4 standard are listed in Table 4. All values in Table 4 are the frequencies corrected to the standard operating conditions using the measured frequency-shift-coefficients in Table 2 for the JILA-145 and for the BIPM-P3 laser<sup>2</sup>. The measured frequency difference between the JILA-145 and BIPM-P3 lasers obtained by the optical heterodyne beat measurement was  $-3.5 \pm 1.6$  kHz. This result was obtained by averaging three different measurement results using a similar setup to that used in Sect. 1 for three different operating parameters. The frequency corrections were made under the standard operating conditions recommended by the CIPM [1] for both lasers. The

<sup>2</sup> The coefficients for the operating parameters of the BIPM-P3 laser, measured in March 2000, are  $-0.048$  kHz/ $\mu\text{W}$ ,  $-9.2$  kHz/MHz, and  $-14.2$  kHz/K, respectively.

**Table 4.** Average frequency differences among three standard lasers participating in the frequency determination of the BIPM-4 standard laser:  $f_{\text{JILA-145}}$ ,  $f_{\text{BIPM-P3}}$ , and  $f_{\text{BIPM-4}}$  are, respectively, the frequencies of the JILA-145 laser, the BIPM-P3 laser, and the BIPM-4 standard laser under standard operating conditions

	Frequency difference (kHz)	Uncertainty (kHz)
$f_{\text{JILA-145}} - f_{\text{BIPM-P3}}$	-3.5	1.6
$f_{\text{BIPM-P3}} - f_{\text{BIPM-4}}$	3.2	0.4
$f_{\text{JILA-145}} - f_{\text{BIPM-4}}$	-0.3	1.65

results of the frequency comparisons between three different laboratories, i.e. the BIPM, JILA, and NRC, are published elsewhere [11]. In order to link the absolute frequency of the JILA-145 laser to that of the BIPM-4 standard laser, it is necessary to know the frequency difference between the BIPM-P3 and BIPM-4 lasers at the standard conditions. The average frequency difference between the BIPM-P3 and BIPM-4 lasers, measured before and after the intercomparison, was  $+3.2 \pm 0.4$  kHz, as shown in Table 4.

The absolute frequency of the JILA-145 laser is linked to the frequency of the BIPM-P3 laser through the frequency intercomparison, which resulted in a direct determination of the absolute frequency of the i component of the BIPM-4 standard laser. By taking into account the frequency difference between the transfer standards (JILA-145 and BIPM-P3) in Table 4 and the absolute frequency of the i component of the JILA-145 laser in (1), we determine the following value for absolute frequency  $f_{i(\text{BIPM})}$  of the i component of the BIPM-4 standard laser:

$$f_{i(\text{BIPM})} = 473\,612\,214\,711.9 \pm 2.0 \text{ kHz}. \quad (2)$$

Although the determined frequency is  $6.9 \pm 2.0$  kHz higher than the internationally accepted value adopted by the CIPM in 1997 [1], it is within the accepted uncertainty of 12 kHz. If we consider the stability (and reproducibility) of the standard lasers involved in the present measurement, however, the accepted uncertainty of 12 kHz may be too generous with regard to the present work, as discussed in Sect. 1. The biggest contribution to the combined measurement uncertainty in (2) is the uncertainty of  $\pm 1.6$  kHz in the frequency-difference measurement between the JILA-145 and BIPM-P3 lasers as shown in Table 4.

### 4 Conclusions

We have measured the absolute frequency of the JILA-145 laser at 633 nm stabilized on the i (or  $a_{13}$ ) component of the 11-5 R(127) hyperfine transition of the  $^{127}\text{I}_2$  molecule using a femtosecond optical comb generator and an iodine-stabilized Nd:YAG laser standard at 1064 nm. The measured frequency of the JILA-145 laser under standard operation conditions is,  $f_{i(\text{JILA})} = 473\,612\,214\,711.57 \pm 1.06$  kHz, which is 6.6 kHz higher than the values adopted by the Comité International des Poids et Mesures (CIPM) in 1997 [1]. From a frequency intercomparison between JILA and the BIPM, we link the absolute frequency of the JILA-145 laser to that of the BIPM-4 standard laser, the as-maintained international iodine-stabilized He–Ne laser standard at 633 nm. The determined absolute frequency of the i component of the BIPM-4 standard laser is  $f_{i(\text{BIPM})} = 473\,612\,214\,711.9 \pm 2.0$  kHz. Our measured frequency for its i component of the BIPM-4 standard laser is 6.9 kHz higher than the internationally accepted value adopted by the CIPM in 1997.

*Acknowledgements.* The work is supported by the National Institute of Standards and Technology and the National Science Foundation. The authors would like to thank S. Diddams and S.T. Cundiff for their contributions to the JILA femtosecond comb generator and are grateful to A. Chartier for her assistance in the frequency intercomparison. In particular, we thank A. Madej for his arrangement and hospitality during the Ottawa intercomparisons. T.H. Yoon acknowledges financial support from JILA.

**References**

1. T.J. Quinn: *Metrologia* **36**, 211 (1999)
2. H. Darnedde, W.R.C. Rowley, F. Bertinotto, Y. Millerieux, H. Haitjema, S. Wetzels, H. Pirée, E. Prieto, M. Mar Pérez, B. Vaucher, A. Chartier, J.-M. Chartier: *Metrologia* **36**, 199 (1999); P. Balling, M. Šmíd, P. Šebek, M. Matus, K. Tomanyiczka, E. Bánréti: *Metrologia* **36**, 433 (1999), and references therein
3. O. Acef, J.J. Zondy, M. Abed, D.G. Rovera, A.H. Gérard, A. Clairon, P. Laurent, Y. Millerieux, P. Juncar: *Opt. Commun.* **97**, 29 (1993)
4. T. Udem, J. Reichert, R. Holzwarth, T.W. Hänsch: *Phys. Rev. Lett.* **82**, 3568 (1999); T. Udem, J. Reichert, R. Holzwarth, T.W. Hänsch: *Opt. Lett.* **24**, 881 (1999)
5. H.R. Telle, G. Steinmeyer, A.E. Dunlop, J. Stenger, D.H. Sutter, U. Keller: *Appl. Phys. B* **69**, 327 (1999)
6. D.J. Jones, S.A. Diddams, J.K. Ranka, A. Stentz, R.S. Windeler, J.L. Hall, S.T. Cundiff: *Science* **288**, 635 (2000)
7. S.A. Diddams, D.J. Jones, L.-S. Ma, S.T. Cundiff, J.L. Hall: *Opt. Lett.* **25**, 186 (2000)
8. S.A. Diddams, D.J. Jones, J. Ye, S.T. Cundiff, J.L. Hall, J.K. Ranka, R.S. Windeler, R. Holzwarth, T. Udem, T.W. Hänsch: *Phys. Rev. Lett.* **84**, 5102 (2000)
9. J. Reichert, M. Niering, R. Holzwarth, M. Weitz, T. Udem, T.W. Hänsch: *Phys. Rev. Lett.* **84**, 3232 (2000)
10. M.S. Taubman, J.L. Hall: *Opt. Lett.* **25**, 311 (2000)
11. J. Ye, T.H. Yoon, J.H. Hall, A.A. Madej, J.E. Bernard, K.J. Siemsen, L. Marmet, J.-M. Chartier, A. Chartier: *Phys. Rev. Lett.* **85**, 3797 (2000)